

This is an Open Access document downloaded from ORCA, Cardiff University's institutional repository: <https://orca.cardiff.ac.uk/id/eprint/142795/>

This is the author's version of a work that was submitted to / accepted for publication.

Citation for final published version:

Kay, William P., Naumann, David S., Bowen, Hannah J., Withers, Simon J., Evans, Benjamin J., Wilson, Rory P., Stringell, Thomas B., Bull, James C., Hopkins, Phil W., Börger, Luca and Gaggiotti, Oscar 2019. Minimizing the impact of biologging devices: Using computational fluid dynamics for optimizing tag design and positioning. *Methods in Ecology and Evolution* 10 (8) , pp. 1222-1233. 10.1111/2041-210X.13216

Publishers page: <http://dx.doi.org/10.1111/2041-210X.13216>

Please note:

Changes made as a result of publishing processes such as copy-editing, formatting and page numbers may not be reflected in this version. For the definitive version of this publication, please refer to the published source. You are advised to consult the publisher's version if you wish to cite this paper.

This version is being made available in accordance with publisher policies. See <http://orca.cf.ac.uk/policies.html> for usage policies. Copyright and moral rights for publications made available in ORCA are retained by the copyright holders.



1 **Minimising the impact of biologging devices: Using Computational Fluid**
2 **Dynamics for optimising tag design and positioning**

3 William P. Kay^{1,2,†,*}, David S. Naumann^{3,*}, Hannah J. Bowen³, Simon Withers³, Benjamin
4 J. Evans³, Rory P. Wilson¹, Thomas B. Stringell⁴, James C. Bull², Phil W. Hopkins¹, Luca
5 Börger¹

6 **Short/Running Title:** Minimising the impact of biologging devices

7

8 **Word count:** 7,999

9 *Both authors contributed equally.

10 †Corresponding author. E-mail: william.p.kay@swansea.ac.uk

11 ¹Swansea Laboratory for Animal Movement, Department of Biosciences, College of
12 Science, Swansea University, Swansea, SA2 8PP, Wales, UK

13 ²Spatial & Population Ecology Research Group, Department of Biosciences, College of
14 Science, Swansea University, Swansea, SA2 8PP, Wales, UK

15 ³Zienkiewicz Centre for Computational Engineering, College of Engineering, Swansea
16 University, SA1 8EN, UK

17 ⁴Natural Resources Wales, Maes y Ffynnon, Penrhos Road, Bangor, Gwynedd, LL57
18 2DW, UK

19

20

21 **Abstract**

- 22 1. Biologging devices are used ubiquitously across vertebrate taxa in studies of
23 movement and behavioural ecology to record data from organisms without the need
24 for direct observation. Despite the dramatic increase in the sophistication of this
25 technology, progress in reducing the impact of these devices to animals is less
26 obvious, notwithstanding the implications for animal welfare. Existing guidelines
27 focus on tag weight (e.g. the '5% rule'), ignoring aero/hydrodynamic forces in aerial
28 and aquatic organisms, which can be considerable. Designing tags to minimise such
29 impact for animals moving in fluid environments is not trivial, as the impact depends
30 on the position of the tag on the animal, as well as its shape and dimensions.
- 31 2. We demonstrate the capabilities of computational fluid dynamics (CFD) modelling to
32 optimize the design and positioning of biologgers on marine animals, using the grey
33 seal (*Halichoerus grypus*) as a model species. Specifically, we investigate the effects
34 of (i) tag form, (ii) tag size and (iii) tag position and quantify the impact under frontal
35 hydrodynamic forces, as encountered by seals swimming at sea.
- 36 3. By comparing a conventional vs. a streamlined tag, we show that the former can
37 induce up to 22% larger drag for a swimming seal; to match the drag of the
38 streamlined tag, the conventional tag would have to be reduced in size by 50%. For
39 the conventional tag, the drag induced can differ by up to 11% depending on the
40 position along the seal's body, whereas for the streamlined tag this difference
41 amounts to only 5%.
- 42 4. We conclude by showing how the CFD simulation approach can be used to optimise
43 tag design to reduce drag for aerial and aquatic species, including issues such as
44 the impact of lateral currents (unexplored until now). We also provide a step-by-step
45 guide to facilitate implementation of CFD in biologging tag design.

46

47 **Second Language Abstract (Welsh)**

48 1. Defnyddir dyfeisiau biogofnodi'n eang iawn ar draws dosbarthiadau fertebrataid
49 mewn astudiaethau symudiad ac ymddygiad ecolegol i gofnodi data o organeddau
50 heb fod angen arsylwi'n uniongyrchol. Er gwaethaf y cynnydd syfrdanol yn natur
51 soffistigedig y dechnoleg hon, mae'r cynnydd wrth leihau effaith y dyfeisiau hyn ar
52 anifeiliaid yn llai amlwg, er gwaethaf y goblygiadau ar gyfer lles anifeiliaid. Mae
53 canllawiau presennol yn canolbwyntio ar bwysau tag (e.e. y 'rheol 5%'), gan
54 anwybyddu grym aero/hydrodynamig mewn organeddau awyr a dyfrol, sy'n gallu bod
55 yn sylweddol. Nid yw dylunio tagiau i leihau effaith o'r fath i anifeiliaid sy'n symud
56 mewn amgylcheddau llifyddol yn beth bach, gan fod yr effaith yn dibynnu ar leoliad
57 y tag ar yr anifail, yn ogystal â'r siâp a'i ddimensiynau.

58 2. Rydym yn dangos galluoedd modelu deinameg hylif gyfrifiannol (CFD) i optimeiddio
59 dyluniad a lleoliad biogofnodwyr ar anifeiliaid morol, gan ddefnyddio'r morlo llwyd
60 (*Halichoerus grypus*) fel rhywogaeth fodel. Yn benodol, rydym yn ymchwilio i
61 effeithiau (i) ffurf y tag, (ii) maint y tag a (iii) lleoliad y tag a meintoli'r effaith dan
62 rymoedd hydrodynameg uniongyrchol, fel y mae morloi sy'n nofio yn y môr yn eu
63 profi.

64 3. Drwy gymharu tag confensiynol â thag llyfn, rydym yn dangos y gall y fersiwn
65 gonfensiynol greu hyd at 22% mwy o effaith lusgo i forlo sy'n nofio; er mwyn efelychu
66 effaith lusgo'r tag llyfn, byddai'n rhaid lleihau maint y tag confensiynol gan 50%. Ar
67 gyfer y tag confensiynol, gall yr effaith lusgo a grëir amrywio hyd at 11%, gan
68 ddibynnu ar ei leoliad ar gorff y morlo, er mai 5% yn unig yw'r gwahaniaeth hwn ar
69 gyfer tag llyfn.

70 4. Rydym yn cloi wrth ddangos sut gall ymagwedd efelychu CFD gael ei defnyddio i
71 optimeiddio dyluniad tagiau a lleihau'r effaith lusgo i rywogaethau awyr a dyfrol, gan
72 gynnwys materion megis effaith cerrynt ystlysol (nad ydynt wedi'u hastudio hyd yma).

73 Rydym hefyd yn cynnig canllaw cam wrth gam i hwyluso rhoi CFD ar waith wrth
74 ddylunio tagiau biogofnodi.

75 **Keywords:** animal welfare, biologging, biotelemetry, computational fluid dynamics, drag,
76 flow simulation, hydrodynamics, tag design

77

78 **1 Introduction**

79 In recent decades, the use of biologging devices to gather information on the behaviour,
80 movement and physiology of animals has increased substantially (Hussey et al. 2015).

81 In addition to collecting vast amounts of movement and behavioural data (Heylen &
82 Nachtsheim 2018), biologging devices can collect oceanographic data (Roquet et al.

83 2017; Treasure et al. 2017), and other environmental measures, such as ambient noise
84 levels (Mikkelsen et al. 2019). However, attachment of devices to animals is not without

85 consequence for the animals carrying them (Thorstad et al. 2001; Vandenabeele et al.
86 2014; Bodey et al. 2017; Wilson et al. 2018). Tag-induced detriment has often been

87 attributed to tag weight (Kenward 2001) which has driven researchers to work within
88 weight-defined bounds (Casper 2009). Indeed, researchers often select their study

89 animals based on the size or weight requirements for the tags, rather than trying to
90 optimise tags for a given species or size class; though there are examples of specific

91 developments made for very small animals (Stidsholt et al. 2018). Despite this, most
92 studies using tags have so far largely failed to take advantage of technological

93 advancements to reduce the impact of tags on animals (Portugal & White 2018).

94 Crucially, for projects involving tags on aerial and aquatic animals, the focus on weight
95 by most existing tag guidelines – e.g. the 3% or 5% rule (Casper 2009) – ignores

96 aero/hydrodynamic impacts (most notably drag) which are key in modulating energy
97 expenditure and behaviour during swimming (Culik & Wilson 1991; Cornick et al. 2006;

98 Rosen et al. 2017; van der Hoop et al. 2018), and flight (Bowlin et al. 2010; Pennycuick
99 et al. 2012; but see Tomotani et al. 2019). This may lead to biased data which is not
100 representative of freely moving animals (Ropert-Coudert et al. 2000; Barron et al. 2010;
101 Lear et al. 2018), as well as raising important ethical concerns for the animal being
102 tagged (Wilson & McMahon 2006).

103 Designing minimal-impact tags and testing drag in real systems is however not trivial, as
104 the impact is a complex function of both the position of the tag on the animal as well as
105 its shape and dimensions (Bannasch et al. 1994; Vandenabeele et al. 2015). One
106 approach to assess the effects of tag-induced drag is by *in-situ* modification of the shape
107 and positioning of tags deployed on a subject animal (or a model of it) in wind or flume
108 tunnels, or in captivity (Culik et al. 1994; van der Hoop et al. 2014; Shorter et al. 2017).
109 These approaches are beneficial insofar as during live experiments it is possible to
110 observe how animals react to tags under real operational conditions (cf. Pavlov &
111 Rashad 2012; van der Hoop et al. 2018), as well as assessing animal energetics, kinetics
112 and biomechanics, and changes in these over time (Geertsen et al. 2004; Ropert-
113 Coudert et al. 2007; Rosen et al. 2017; van der Hoop et al. 2018). However, experimental
114 approaches are limited in that they are very time consuming and labour intensive, wind
115 or flume tunnels are not always accessible, and the use of live animals raises ethical
116 concerns and requires appropriate licensing (Kyte et al. 2018). Furthermore, the logistical
117 constraints of working with very large taxa (e.g. cetaceans) often make *in-situ*
118 experiments impractical.

119 An alternative to experimental approaches uses computational fluid dynamics (CFD) to
120 assess tag-induced drag (Kyte et al. 2018). CFD is the primary tool for virtual design and
121 drag modelling within the aerospace industry (Jameson & Vassberg 2001) and is notable
122 in being able to model drag with the accuracy of results comparable to physical
123 experiments (Tyagi & Sen 2006; Jagadeesh et al. 2009; Vassberg et al. 2014); for

124 example Shorter et al. (2014) demonstrated that CFD simulation predictions of tag-
125 induced drag agreed with experimental assessments. Of particular value is that CFD
126 analysis can be implemented quickly and efficiently and can gather repeated,
127 comprehensive measures on aero/hydrodynamic aspects of tag design. As such, CFD
128 analysis can aid the prototyping of biologging tags prior to manufacture by estimating
129 their effects in a virtual environment without the need for experiments (Pavlov et al. 2007;
130 Kyte et al. 2018). Indeed, CFD has the potential to revolutionise biologging tag design
131 (Heylen & Nachtsheim 2018).

132 The use of CFD to examine tag design and impact has grown within the biologging
133 community since the mid-2000s (Pavlov et al. 2007) (see appendix S1 for a brief review).
134 Some commercial tag manufacturers utilise CFD to assess tags during product
135 development, though results from these studies are often not published. Indeed, the use
136 of CFD to examine tag-induced drag remains relatively limited in peer-reviewed
137 literature, and its full potential may not yet have been realised. Specifically, while there
138 have been several advances in the use of CFD to design tags and quantify their impact
139 (appendix S1), no publication has yet examined an approach which simultaneously
140 considers device size (Vandenabeele et al. 2015), shape (Shorter et al., 2014) and
141 positioning along the animal's body (Bannasch et al. 1994; Vandenabeele et al. 2014).

142 It is important to note that while the use of CFD to assess tag-induced drag is an
143 increasingly popular method, with clear advantages over experimental alternatives (Kyte
144 et al. 2018), it does have limitations, and one of our aims is to help ecologists become
145 aware of these and efficiently deal with them. Briefly, CFD analysis can be sensitive to
146 the choice of turbulence model; results may be specific to the particular tag and animal
147 geometries used in the study (thus care is required to compare results from different
148 studies); and geometric simplifications (such as the removal of antenna) are often

149 required during modelling, which will affect results. Further details of these limitations are
150 covered in appendix S2.

151 Nevertheless, provided potential limitations are acknowledged, CFD is an excellent tool
152 to test hypotheses at the level of concept (Pavlov & Rashad 2012), particularly if the aim
153 is, as is often the case (including in this study), to compare the drag of tagged versus
154 untagged animals, and to assess the effect of various designs, sizes and positions of
155 tags. CFD software is freely available for researchers, but its use has been largely
156 restricted to commercial tag manufacturers, individuals with substantial prior expertise,
157 or teams who are able to collaborate with aerospace engineers (Kyte et al. 2018).
158 Conversely, novice CFD users, like many ecologists, are not routinely able to implement
159 such techniques themselves.

160 Here we address this gap and support ecologists to realise the full potential of CFD for
161 improving tag design and assessing tag-induced drag. Specifically, we (i) evaluate how
162 tag-induced drag varies with device shape, size and positioning on the animal, (ii)
163 exemplify the efficacy of CFD for tag design, and (iii) provide step-by-step instructions
164 for ecologists to use CFD to efficiently assess the drag impact of biologging tags
165 (appendix S3); facilitating effective, future interdisciplinary collaborations with engineers.

166 **2 Materials and Methods**

167 In addition to this section, we provide a step-by-step guide to modelling the drag impact
168 of tags with CFD simulations using ANSYS FLUENT™, version R15.0 (ANSYS, Inc.,
169 Pennsylvania, USA) (appendix S3).

170 **2.1 Construction of geometries**

171 We used computer aided design (CAD) software (Autodesk® Inventor LT™, Autodesk
172 Inc., California, USA) to construct and manipulate seal and tag geometries. Note that

173 any modern 3D CAD software package will allow the geometric manipulations necessary
174 to reproduce this work. For the purpose of this study, two tag geometries were
175 considered. The first represented a traditional GPS tag for seals (tag A), as used in
176 Hazekamp et al. (2010), measuring 10 x 7 x 4 cm (length x width x height). The second
177 geometry represented a streamlined tag designed by us (tag B), measuring 11 x 10 x 4
178 cm. Both tags were designed to contain multiple biologging sensors capable of recording
179 data on seal movements and behaviour.

180 The seal geometry was obtained from Hazekamp et al. (2010) in IGES (.igs) format and
181 converted into a solid body for integration with the tag geometries. We chose to use the
182 seal and tag A geometries from Hazekamp et al. (2010) in order to facilitate direct
183 comparison of results. Importantly, the results from CFD simulations (see later) will
184 depend on (and be specific to) the chosen size of the animal geometry, hence the
185 geometry should be an appropriate reflection of the real animal being studied. Our seal
186 geometry was 1734 mm long – within the range of a typical adult female grey seal
187 (McLaren 1993). Our main aim was to exemplify the CFD method by assessing effects
188 of size, shape and position of the main body design of two tags on induced drag. Hence,
189 to maintain simplicity in the CFD modelling (cf. Kyte et al. 2018), external features such
190 as the antennae were removed from both tag geometries (see appendices S2 and S4
191 for details).

192 To prepare the geometries ahead of export to the CFD mesh generation process, we
193 used CAD ‘cleaning’ software (CADfix, International TechneGroup, Inc., Ohio, USA) to
194 ensure that the combined seal-tag solid body was ‘watertight’. This is necessary to allow
195 the subsequent modelling of drag effects of the tag at different positions along the
196 animal’s body.

197 **2.2 CFD simulations**

198 We undertook mesh generation, pre-processing and CFD simulations also within ANSYS
199 Fluent™. We first undertook a mesh convergence study to determine the appropriate
200 mesh resolutions required for the simulations. We generated a surface mesh (Fig. 1),
201 encompassing the seal body and tag, composed of a finely resolved mesh for the fluid
202 boundary layer around the seal (Fig. 1 (a)), and a further (coarser) volume mesh for the
203 remainder of the volume around the seal body (Fig. 1(b)) (see appendix S4 for further
204 details). The surface mesh provided the input to ANSYS Fluent's numerical solver to
205 simulate the flow and determine flowfield properties, such as turbulence, around the
206 animal body under different freestream conditions, and to compute force coefficient
207 outputs. Importantly, the assumption was made that a steady-state solution existed for
208 each (non-dynamic) case, which allows for local time integration within the CFD solver,
209 as a precise time history of the solution was not necessary.

210 Flow visualisations were obtained using the software package *EnSight* and ANSYS
211 PostProcessing (ANSYS, Inc., Pennsylvania, USA), to provide a qualitative description
212 of the underlying fluid dynamics causing the force coefficient responses observed. A
213 summary of the CFD process is provided in Fig. 2 (and refer to appendix S4 for specific
214 details; see also appendix S3).

215 Simulations were undertaken using a range of flow speeds (1, 3, 5, 7 and 9 ms⁻¹) within
216 the typical range for simulation approaches for seals, including resultant speeds
217 encountered when seals swim into an oncoming flow, e.g. in high tidal flow environments
218 (Hazekamp et al. 2010; Kyte et al. 2018; Hastie et al. 2019). We computed non-
219 dimensional force coefficients in order to verify that non-dimensionalised outputs were
220 insensitive to the absolute input freestream velocity across this range; indeed, all force
221 coefficients collapsed onto a single curve across this speed range, indicating that the
222 force coefficient response was independent of freestream speed, and that our results
223 remained consistent across the range of velocities modelled. Thus, a velocity of 5 ms⁻¹

224 was selected for further investigation because we were particularly interested in the drag
225 effects and performance of tags when flow speed was relatively high; such speeds may
226 be encountered by seals swimming in highly tidal, fast flowing areas (Hastie et al. 2019).
227 In line with Pavlov & Rashad (2012) our model was assumed to represent an animal
228 swimming at a constant speed in a rectilinear fashion. While at sea, seals undertake a
229 range of complex 3D motions (Mitani et al. 2003) and move at varying speeds (Williams
230 2018). Hence, our results cannot account for the full range of movement that a seal
231 exhibits, but instead focus on the predominant forward motion of straight line swimming
232 that seals undertake during transit (Davis et al. 2001). These simplifications are
233 necessary due to the added complexity of modelling the highly unsteady and interacting
234 effects of fluid flow around a non-rigid, moving body (Adkins & Yan 2006); while these
235 analyses are possible and certainly interesting for future studies, they require the use of
236 unsteady, fluid-structure interaction CFD modelling techniques (Adkins & Yan 2006) and
237 were unnecessary for our aims (see also Kyte et al. 2018).

238 The output from the CFD simulations was the non-dimensional drag coefficient (C_d) for
239 each seal and tag combination. The Reynolds number, Re , of the flow simulations,
240 defined as

$$241 \quad Re = \frac{\rho VL}{\mu} \quad (1)$$

242 where ρ is the fluid density (1028 kg m^{-3}), V is the freestream flow velocity (5 m s^{-1}), L is
243 the seal length (1734 mm) and μ is the dynamic viscosity of salt water ($1.09 \times 10^{-3} \text{ Pa s}$),
244 was 8.2×10^6 .

245 All non-dimensional drag coefficients, C_d , defined as

$$246 \quad C_d = \frac{D}{\frac{1}{2}\rho V^2 A} \quad (2)$$

247 where D is the absolute drag value (in Newtons) of each seal and tag combination, were
248 determined for each tag type, at nine discrete positions along the seal's dorsal surface,
249 under frontal flow (zero angle of attack) using the seal frontal area, A (0.134 m^2), as the
250 reference. The nine positions studied ranged from the seal's neck (position 1; 216 mm
251 from the nose) to 1080 mm from the nose (position 9) (Fig. 3). The comparisons of C_d
252 values are for the combined seal-tag body.

253 **2.3 The effect of tag size, shape and position on tag-induced drag**

254 To examine the effect of tag size, we used the non-dimensional drag coefficient (C_d),
255 hereon "drag", obtained from the CFD solver, to predict by how much the standard tag
256 (A) would need to be decreased in size in order to reduce its absolute drag penalty to
257 the same value of the more hydrodynamic tag B (under the same flow conditions). Thus,
258 via a process of linear re-scaling, we iteratively reduced the size of tag A to reach the
259 equivalent drag penalty to that of tag B.

260 We used a paired t-test to examine the effect of tag shape on tag-induced drag (i.e. mean
261 drag over the full range of nine positions modelled). To test the effect of tag positioning
262 *per se* we modelled drag as a function of position using a linear fixed-effects model (using
263 a cubic polynomial function to account for the non-linear effect of position), including tag
264 type (A or B) as a fixed effect (to account for shape effects), interacting with position. We
265 used step-wise model selection to compare the full model (with an interaction between
266 tag shape and position) vs the intercept only model, as well as comparing cubic vs
267 quadratic polynomial functions for the position covariate, retaining the former in both
268 cases. All analyses were performed using R version 3.5.1 (R Core Team 2018).

269 **3 Results**

270 We used CFD modelling to quantify the drag increase of tags on marine animals over
271 the baseline case of a non-tagged animal, using the grey seal as a model species. The
272 results presented in this section outline the effects of shape, size and positioning of two
273 contrasting tag types on the turbulence and pressures generated around the tag, and
274 hence the drag experienced by tagged animals.

275 **3.1 Turbulence and pressures generated by tags with contrasting shape**

276 Tag A, a standard tag, commonly used for seals and other marine mammals, with a non-
277 streamlined shape, induced considerably more turbulent distortions, particularly in the
278 wake of the device, than the streamlined tag B, with the reattachment point of the lowest,
279 smooth streamline passing over tag A 20% further downstream from the base of the tag
280 than in the case of tag B (Fig. 4). This delayed reattachment of streamlined flow results
281 in a turbulent wake region that is approximately 30% larger (when viewed transversely).
282 This type of drag is often referred to as 'base drag' (Suliman et al. 2009) and is one of
283 the major contributors to the increased drag of tag A. There are also stagnant, turbulent
284 flow regions on the upper side of tag A which are not evident on tag B (Fig. 4). These
285 stagnant regions (due to the less streamlined upper surface of tag A) contribute to
286 increased drag. The peak pressure on the front of tag A is 15% higher than that on tag
287 B and the high pressure region on tag A (see red area in Fig. 4) is 65% larger than that
288 on tag B. There is also evidence of a considerable low pressure (blue) region, generating
289 suction, on the upper surface of tag A which is not present on tag B. The general form of
290 the regions of high and low pressure across the tags was consistent across all positions
291 for both tag shapes (Fig. 4).

292 **3.2 Shape and size effects on drag experienced by tagged animals**

293 Tag A produced an 18.5% greater mean percentage drag increase than tag B across the
294 full range of positions studied ($t = 16.012$, $df = 8$, $p < 0.001$) (Table 1), with a maximum

295 percentage increase of 22.3% greater than tag B (at position 6) (Table 2). These results
296 mean that tag A would require a ca. 50% linear scaling reduction in size to reduce its
297 drag penalty to that of tag B; i.e. from 10 x 7 x 4 cm (c.f. Table 1) to 5 x 3.5 x 2 cm. It is
298 also worth noting that tag B is the preferred option for lower absolute drag despite it being
299 markedly larger than tag A.

300 **3.3 Position effects on drag experienced by tagged animals**

301 The positioning of tags had a marked impact on their drag (Fig. 5) (Tag A: $F_3 = 25.253$,
302 $p < 0.001$; Tag B: $F_3 = 10.362$, $p < 0.001$). Positions 2 and 9 (on the dorsal surface at the
303 neck, and between the shoulder blades respectively; corresponding to 215.75 mm and
304 1083.44 mm from the tip (nose) of the model), were optimum for tag A and tag B,
305 respectively (Fig. 5). The drag varied non-linearly with positioning, and this effect differed
306 by tag type ($p = 0.002$). Drag was greatest around the mid-point of the dorsal surface on
307 the model seal (specifically, positions 5 and 6 for tag A, and positions 3 and 4 for tag B)
308 (Fig. 5; Table 2). Importantly, the variability in tag-induced drag between attachment
309 positions was markedly greater in tag A, with drag values ranging from 0.071 to 0.078;
310 equating to an increase in drag penalty, compared to a seal with no tag, of +20.8% to
311 +32.1%, with a maximum drag penalty difference of 11.3% between positions 2 and 6.
312 For tag B these values ranged from 0.063 to 0.066, equating to an increase in drag of
313 +6.5% to +11.9%, with a maximum difference of 5.4% between positions 4 and 9 (Table
314 2). Accordingly, the coefficient of variation in drag for tag A (3.31 %) was almost double
315 that of tag B (1.71 %).

316 **4 Discussion**

317 We showed how CFD modelling can be used to quantify and reduce tag impact on
318 aquatic and aerial animals through virtual design testing. Using the example of tags
319 attached to grey seals, we showed how to evaluate and quantify the interacting effects

320 of tag shape, size and position on the magnitude of tag-induced drag. Our step-by-step
321 guide (appendix S3) provides a standardised framework for ecologists to use CFD to
322 assess the drag impact of tags, and more routinely report it in publications.

323 Tag A gave rise to a more turbulent flow disturbance, which also propagated over a
324 longer distance, than for tag B (Fig. 4). This contributed to the greater drag generated by
325 tag A (Table 1; 2). This increase in drag can also be attributed to the larger regions of
326 high (red) and low (blue) pressure differentials than for tag B (Fig. 4). This is in
327 accordance with other CFD and wind tunnel research on seals (Kyte et al., 2018),
328 cetaceans (Fiore et al. 2017) and birds (Vandenabeele et al. 2014), where greater
329 turbulent flow distortions and larger pressure differentials contributed to increased drag.
330 We note that the absolute drag values observed in our study are larger than those
331 obtained in Kyte et al. (2018), who modelled tag-induced drag on a similarly sized harp
332 seal. This can be attributed to the large difference in flow velocities used in the
333 simulations; Kyte et al. (2018) used a maximum flow velocity of 1.7 ms^{-1} whereas our
334 simulations used 5 ms^{-1} . Importantly, when scaled to non-dimensional drag, our values
335 are in line with that work. Likewise, when comparing our work to Hazekamp et al. (2010)
336 we found similar yet quantitatively different results. Specifically, Hazekamp et al. (2010)
337 observed a 13.8% increase in drag, whereas we saw an increase of 23.5%. This
338 difference is expected because Hazekamp et al. (2010) ran their simulations using the
339 $k-\epsilon$ turbulence model, which tends to underpredict the drag impact of a tag (see Kyte et
340 al. 2018 and appendix S2 for further details).

341 Tag A had a considerably larger low pressure region than tag B (Fig. 4) which could
342 negatively impact tagged animals by contributing to a lift force trying to pull the tag off
343 the animal (Fiore et al. 2017). High and low pressure differentials can act to increase
344 shear loading or downforce, which could cause injury at the site of attachment, or lead
345 to early detachment of a tag from an animal (Fiore et al. 2017). Hence, minimising drag

346 will likely also increase attachment time for suction cup tags (Pavlov et al. 2007; Fiore et
347 al. 2017). CFD modelling can also resolve lift forces and we note that both tags generated
348 substantial variation in lift coefficient (C_l) (Table 2), although the magnitude of C_l was
349 negligible compared to the drag. It was not a primary aim of ours to investigate C_l , hence
350 we reserve discussion of this to the supporting information (appendix S5).

351 Our comparison of two contrasting tag designs allowed us to exemplify that tag shape
352 may be more influential than size *per se* in generating increased drag for tagged animals,
353 with the considerably larger but more hydrodynamically designed tag (B) giving rise to a
354 lower drag penalty than the smaller tag A (Table 1). This result is in agreement with
355 Balmer et al. (2014) who demonstrated that the size of tags was an insignificant driver
356 of overall drag, with only a 1.2% increase in drag between the smallest (25 mm) and
357 largest (38.6 mm) tags studied. Thus, we propose that tag shape should be considered
358 more systematically (Fig 5-6) and we demonstrated how CFD simulations are ideal for
359 this. Moreover, achieving the reduction in size that would be necessary to reduce drag
360 without instead designing a more streamlined form (here a reduction in size of tag A by
361 ca. 50 %) is often not possible due to limitations in the size of electronic components and
362 batteries. On the contrary, our results suggest there may be scope to increase the size
363 of tags, within reason, providing that their form ultimately leads to a reduction in drag
364 (Fig. 6) – see also Shorter et al. (2014) and Fiore et al. (2017). Certainly, seen in this
365 light, the persistent stated aim to simply "miniaturise" biologging devices may be too
366 simplistic (Portugal & White 2018).

367 If tag size is to be increased, other factors such as minimizing the area of contact with
368 the animal (i.e. tag footprint) or the method of tag attachment must also be considered
369 (Shorter et al. 2014). This is because the direct attachment of tags to study animals has
370 been shown to disrupt thermoregulatory responses, or create superficial abrasions
371 (McCafferty et al. 2007; Field et al. 2012). For example, tags attached to juvenile grey

372 seals gave rise to a 23% greater heat-flux where devices were attached, compared to
373 areas of undisturbed fur, which was likely due to heat leakage around the attachment
374 site (McCafferty et al. 2007). Superficial abrasions were observed when tags were
375 attached to seals using a mesh attachment (Mazzaro & Dunn 2010), and the use of
376 epoxies to attach external devices to the pelage of animals has the potential to cause
377 burns at the site of attachment (Field et al. 2012). Larger tags, if attached by these
378 methods, would require larger meshes and greater quantities of epoxy. Hence,
379 minimising tag footprint is important, and this further exemplifies the usefulness of using
380 CFD to efficiently and quickly evaluate the pros and cons of different tag design and size
381 choices. It is also important to note that the effect of tag-induced drag is likely to be
382 greater as the ratio of tag to animal volume increases (Kyte et al. 2018), and minimising
383 tag frontal cross-sectional area should also be undertaken where possible (Rosen et al.
384 2017). Ultimately, to reduce drag, tags should be designed to be more streamlined in
385 line with the contours of the animal being tagged, to achieve smooth flow reattachment
386 downstream of the tag (see tag B; Fig. 4). For this, an increase in size (and thus volume
387 and/or cross-sectional area) could be justified.

388 We demonstrated that device positioning is crucial in determining tag-induced drag, as
389 evidenced by the non-linear relationship between drag and tag position (Fig. 5). This
390 concurs with the results of Vandenabeele et al. (2014) who observed strong and non-
391 linear effects of tag position on induced drag on a model cormorant in a wind tunnel.
392 Similarly, Tudorache et al. (2014) documented that for swimming eels tagged with
393 biologging devices, placement of a tag in a non-optimum position, compared to an
394 optimum position, could result in a 15% reduction in critical swimming speed and a
395 significant increase in oxygen consumption rate while swimming. Our results also
396 showed that the effect of tag positioning on drag is significantly dependent upon the
397 shape of the tag, and that the variability in the effect of tag positioning for tag B is almost

398 half that for tag A. This demonstrates that improving hydrodynamic design can reduce
399 the impact of positioning *per se* on device-induced drag.

400 In practice, the choice of tag positioning will also depend on the form of the animal and
401 is further compounded by the fact that the positioning of a tag can affect both the quality
402 and quantity of data collected (Watson & Granger 1998; Jones et al. 2011). For example,
403 GPS data from marine animals can only be obtained when individuals surface for a long
404 enough duration to receive a satellite fix, and for this reason tags are routinely placed on
405 areas of the animal that are exposed most frequently and for the longest periods, for
406 example on the head of pinnipeds (Lake et al. 2006). This is pertinent also for
407 researchers deploying satellite transmitting devices with the aim of maximising the
408 number of successful transmissions, such as uplinks to the Argos network (Service
409 Argos, Toulouse, France). In such cases it may be that the optimum position of the tag
410 for data acquisition or transmission purposes could well be the least suitable position for
411 minimising drag (Watson & Granger 1998; Jones et al. 2011). In such cases, researchers
412 must consider the trade-offs of successful data acquisition with device effects, or
413 consider how they might modify their tags to achieve a more desirable outcome (Jones
414 et al. 2011); for example, researchers could consider using alternative technologies,
415 such as Fastloc-GPS devices, that require only very short durations at the surface (< 1
416 s) to acquire satellite fixes (Dujon et al. 2014), so that tags can be placed at optimum
417 (i.e. drag-minimising) positions on the animal that are exposed for shorter durations. The
418 method of attachment will also determine how accurately the tag can be positioned and
419 orientated on the animal. For example, tags that are attached by hand (such as tags
420 glued to seals) can be positioned more accurately than a tag attached using a pole e.g.
421 to a cetacean, (Stimpert et al. 2013). The position of tags may also shift during their
422 attachment period (e.g. suction cup tags). CFD offers the opportunity to explore the effect

423 of drag of tags positioned anywhere and in any orientation on the subject animal (Fiore
424 et al. 2017).

425 Tag position also affects the signals that are recorded - consider for example an
426 accelerometer: the signal received from a device placed on the head will be very different
427 to that of the same device placed on the back of an animal, given that accelerometers
428 are sensitive to tag orientation (Shepard et al. 2008). This factor would likely also play a
429 part in determining the final choice of device positioning. Managing these trade-offs is
430 challenging and requires that ecologists understand the behaviour of their study species
431 and the functioning of their tag, so that they can make appropriate decisions about where
432 to position a device and understand the drag-impacts of their choices (Jones et al. 2011);
433 this can be fully explored for different species and different devices using CFD.

434 Projects involving tag deployments are diverse and it is not always possible for
435 researchers to rely solely on “off-the-shelf” tags purchased from commercial companies,
436 with many researchers instead resorting to building their own (Kwok 2017). However,
437 there is currently limited advice for researchers who are developing their own tags about
438 how to quantify the drag of their tags and hence how to minimise impact. Here, we fill
439 this gap by providing a step-by-step guide that ecologists can follow to assess tag-
440 induced drag in a quick and efficient manner using CFD techniques (appendix S3), which
441 will aid more researchers to report on the drag-impact of their tags. The guide is written
442 for use with the standard CFD software ANSYS Fluent, used also by other ecologists
443 (Pavlov et al. 2007; Hazekamp et al. 2010), and guides users through the process of
444 modelling the drag impact of tags, from importing the tag design and animal geometry
445 files into the software, through setting up the computational environment and on to
446 running the CFD simulations. The guide will also help in establishing interdisciplinary
447 collaborations with engineers, and aid researchers across the biologging community to
448 increase their understanding of tag-induced drag and work towards best practices in tag

449 design, without the need to rely on collecting logistically challenging empirical data, for
450 example through the use of wind tunnel experiments (Vandenabeele et al. 2014).

451 In this study, we have focused on measuring drag with respect to frontal flow, i.e. a rigid
452 (or stationary) seal in a field of non-turbulent water (steady-state assumption), including
453 at different flow velocities. This modelling approach can be extended to consider lateral
454 flow, as seals also perform turns or may swim at an angle relative to water current (and
455 in doing so can experience lateral hydrodynamic drag forces). Note that this is different
456 to changing the orientation of the tag on the animal, as demonstrated by Shorter et al.
457 (2014). The drag forces incurred by tags are likely to change markedly in each of these
458 circumstances and hence are also important to bear in mind. Such investigations can be
459 undertaken with a simple extension of our step-by-step guide, by rotating the model
460 animal in the computational environment so that it is lateral to the oncoming flow (see
461 appendix S6 for a first investigation of this).

462 The CFD method presented here offers a quick and efficient way to determine the best
463 tag (for reducing drag) for the animal being studied, by considering multiple factors
464 including tag design, size and position. However, researchers planning on using CFD
465 must be aware of its limitations. CFD relies on approximate, numerical solutions to the
466 governing fluid dynamic equations, and so there will always be some discrepancies in
467 absolute force predictions between independent studies; we have highlighted some key
468 comparisons between our results and those of similar works (Hazekamp et al. 2010; Kyte
469 et al. 2018). We provide necessary further detail on the limitations of CFD in appendix
470 S2, which we encourage the reader to consult for guidance.

471 This work has demonstrated the value of an interdisciplinary approach, harnessing
472 engineering techniques to design minimal impact tags and efficiently assess their relative
473 drag loading. While CFD has previously been utilised to measure the impact of tags

474 (appendix S1), its use has largely been limited to researchers with substantial prior CFD
475 modelling expertise (Kyte et al. 2018). The methods we use here are standard for
476 aeronautical design (Jameson & Vassberg 2001) and our guide offers new opportunities
477 for further collaboration between engineers and ecologists - particularly for researchers
478 novice to CFD techniques.

479 Finally, most existing guidelines for tag impact do not advise on appropriate tag size,
480 placement positions or configurations (Rosen et al. 2017) and many are relatively naïve
481 to the impacts of drag that are most relevant to marine and aerial applications (see
482 appendix S7 for an overview). We anticipate that the reporting of drag values in future
483 publications may help improve future guidelines and address recent requests in the
484 literature for improved reporting of impacts (Bodey et al. 2017; Lameris & Kleyheeg 2017)
485 and better assessment of tag-induced effects (such as drag) prior to deployment in the
486 field (Lear et al., 2018). Whilst we do not expect our findings to be taken up as formal
487 guidelines, nor the use of CFD to be made compulsory, we hope that this work, and
488 specifically our step-by-step guide (appendix S3), will aid the biologging community in
489 achieving this.

490 **Acknowledgements**

491 We thank Dr. Roy Mayer who provided the CAD files for the seal and tag A geometries,
492 and the permission for their use. We thank two anonymous reviewers and the associate
493 editor for their helpful comments which improved the manuscript. WPK is supported by
494 the Welsh Government's European Social Fund (ESF), Natural Resources Wales (NRW)
495 and SEACAMS2. The authors declare no conflict of interest.

496 **Author Contributions**

497 WPK, DSN, BJE, RPW, LB, TBS, JCB conceived and designed the research; DSN, BJE,
498 HB, SW and WPK undertook the analyses, with feedback from WPK, LB and RPW. WPK
499 led the writing of the manuscript. DSN, BJE, HB and SW wrote the step-by-step guide to
500 running the CFD simulations. PH created the tag B geometry. LB, RPW, DSN, BJE, JCB
501 and TBS contributed critically to manuscript drafts. All authors gave final approval for
502 publication.

503 **Data Accessibility**

504 Data are available from figshare: <https://doi.org/10.6084/m9.figshare.8152943>. These
505 data are under embargo until 1 August 2019.

506 **References**

- 507 Adkins, D., & Yan, Y. Y. (2006). CFD simulation of fish-like body moving in
508 viscous liquid. *Journal of Bionic Engineering*, 3(3), 147–153.
- 509 Balmer, B. C., Wells, R. S., Howle, L. E., Barleycorn, A. A., McLellan, W. A.,
510 Ann Pabst, D., ... Zolman, E. S. (2014). Advances in cetacean telemetry: A
511 review of single-pin transmitter attachment techniques on small cetaceans
512 and development of a new satellite-linked transmitter design. *Marine*
513 *Mammal Science*, 30(2), 656–673.
- 514 Bannasch, R., Wilson, R. P., & Culik, B. (1994). Hydrodynamic aspects of
515 design and attachment of a back-mounted device in penguins. *The Journal*
516 *of Experimental Biology*, 194(1), 83–96.
- 517 Barron, D. G., Brawn, J. D., & Weatherhead, P. (2010). Meta-analysis of
518 transmitter effects on avian behaviour and ecology. *Methods in Ecology*

- 519 *and Evolution*, 1(2), 180–187.
- 520 Bodey, T. W., Cleasby, I. R., Bell, F., Parr, N., Schultz, A., Votier, S. C., &
521 Bearhop, S. (2017). A Phylogenetically Controlled Meta-Analysis of
522 Biologging Device Effects on Birds: Deleterious effects and a call for more
523 standardized reporting of study data. *Methods in Ecology and Evolution*,
524 12(10), 3218–3221.
- 525 Bowlin, M. S., Henningsson, P., Muijres, F. T., Vleugels, R. H. E., Liechti, F., &
526 Hedenström, A. (2010). The effects of geolocator drag and weight on the
527 flight ranges of small migrants. *Methods in Ecology and Evolution*, 1(4),
528 398–402.
- 529 Casper, R. M. (2009). Guidelines for the instrumentation of wild birds and
530 mammals. *Animal Behaviour*, 78(6), 1477–1483.
- 531 Cornick, L. A., Inglis, S. D., Willis, K., & Horning, M. (2006). Effects of increased
532 swimming costs on foraging behavior and efficiency of captive Steller sea
533 lions: Evidence for behavioral plasticity in the recovery phase of dives.
534 *Journal of Experimental Marine Biology and Ecology*, 333(2), 306–314.
- 535 Culik, B. M., Bannasch, R., & Wilson, R. P. (1994). External devices on
536 penguins: How important is shape? *Marine Biology*, 118, 353–357.
- 537 Culik, B., & Wilson, R. P. (1991). Swimming energetics and performance of
538 instrumented adelic penguins (*Pygoscelis adeliae*). *Journal of Experimental*
539 *Biology*, 158, 355–368.
- 540 Davis, R. W., Fuiman, L. A., Williams, T. M., & Le Boeuf, B. J. (2001). Three-

541 dimensional movements and swimming activity of a northern elephant seal.
542 *Comparative Biochemistry and Physiology - A Molecular and Integrative*
543 *Physiology*, 129(4), 759–770.

544 Dujon, A. M., Lindstrom, R. T., & Hays, G. C. (2014). The accuracy of Fastloc-
545 GPS locations and implications for animal tracking. *Methods in Ecology*
546 *and Evolution*, 5(11), 1162–1169.

547 Field, I. C., Harcourt, R. G., Boehme, L., De Bruyn, P. J. N., Charrassin, J. B.,
548 McMahon, C. R., ... Hindell, M. A. (2012). Refining instrument attachment
549 on phocid seals. *Marine Mammal Science*, 28(3), 325–332.

550 Fiore, G., Anderson, E., Garborg, C. S., Murray, M., Johnson, M., Moore, M. J.,
551 ... Shorter, K. A. (2017). From the track to the ocean: Using flow control to
552 improve marine bio-logging tags for cetaceans. *PLoS ONE*, 12(2), 1–19.

553 Geertsen, B. M., Teilmann, J., Kastelein, R. A., Vlemmix, H. N. J., & Miller, L. A.
554 (2004). Behaviour and physiological effects of transmitter attachments on a
555 captive harbour porpoise (*Phocoena phocoena*). *Journal of Cetacean*
556 *Research and Management*, 6(2), 139–146.

557 Hastie, G. D., Bivins, M., Coram, A., Gordon, J., Jepp, P., MacAulay, J., ...
558 Gillespie, D. (2019). Three-dimensional movements of harbour seals in a
559 tidally energetic channel: Application of a novel sonar tracking system.
560 *Aquatic Conservation: Marine and Freshwater Ecosystems*,
561 doi:10.1002/aqc.3017

562 Hazekamp, A. A. H., Mayer, R., & Osinga, N. (2010). Flow simulation along a

- 563 seal: The impact of an external device. *European Journal of Wildlife*
564 *Research*, 56(2), 131–140.
- 565 Heylen, B. C., & Nachtsheim, D. A. (2018). Bio-telemetry as an essential tool in
566 movement ecology and marine conservation. In *YOUMARES 8–Oceans*
567 *Across Boundaries: Learning from each other* (pp. 83-107). Springer,
568 Cham.
- 569 Hussey, N. E., Kessel, S. T., Aarestrup, K., Cooke, S. J., Cowley, P. D., Fisk, A.
570 T., ... Whoriskey, F. G. (2015). Aquatic animal telemetry: A panoramic
571 window into the underwater world. *Science*, 348(6240), 1255642.
- 572 Jagadeesh, P., Murali, K., & Idichandy, V. G. (2009). Experimental investigation
573 of hydrodynamic force coefficients over AUV hull form. *Ocean Engineering*,
574 36, 113–118.
- 575 Jameson, A., & Vassberg, J. (2001). Computational fluid dynamics for
576 aerodynamic design: Its current and future impact. In *39th Aerospace*
577 *Sciences Meeting and Exhibit*, p. 538.
- 578 Jones, T., Bostrom, B., Carey, M., Imlach, B., Mikkelsen, J., Ostafichuk, P., ...
579 Jones, D. (2011). Determining Transmitter Drag and Best-Practice
580 Attachment Procedures for Sea Turtle Biotelemetry. *NOAA Technical*
581 *Memorandum, NMFS-SWFSC*.
- 582 Kenward, R. (2001). *A manual for wildlife radio tagging*. Academic Press.
- 583 Kwok, R. (2017). Field Instruments: Build it yourself. *Nature*, 545(7653), 253–
584 255.

- 585 Kyte, A., Pass, C., Pemberton, R., Sharman, M., & McKnight, J. C. (2018). A
586 computational fluid dynamics (CFD) based method for assessing the
587 hydrodynamic impact of animal borne data loggers on host marine
588 mammals. *Marine Mammal Science*, doi:10.1111/mms.12540
- 589 Lake, S., Burton, H., & Wotherspoon, S. (2006). Movements of adult female
590 Weddell seals during the winter months. *Polar Biology*, 29(4), 270–279.
- 591 Lameris, T. K., & Kleyheeg, E. (2017). Reduction in adverse effects of tracking
592 devices on waterfowl requires better measuring and reporting. *Animal*
593 *Biotelemetry*, 5(1), 24.
- 594 Lear, K. O., Gleiss, A. C., & Whitney, N. M. (2018). Metabolic rates and the
595 energetic cost of external tag attachment in juvenile blacktip sharks
596 *Carcharhinus limbatus*. *Journal of Fish Biology*, 93(2), 391–395.
- 597 Mazzaro, L. M., & Dunn, J. L. (2010). Descriptive account of long-term health
598 and behavior of two satellite-tagged captive harbor seals *Phoca vitulina*.
599 *Endangered Species Research*, 10(1), 159–163.
- 600 McCafferty, D. J., Currie, J., & Sparling, C. E. (2007). The effect of instrument
601 attachment on the surface temperature of juvenile grey seals (*Halichoerus*
602 *grypus*) as measured by infrared thermography. *Deep-Sea Research Part*
603 *II: Topical Studies in Oceanography*, 54(3–4), 424–436.
- 604 McLaren, I. A. (1993). Growth in pinnipeds. *Biological Reviews*, 68(1), 1–79.
- 605 Mikkelsen, L., Johnson, M., Wisniewska, D. M., van Neer, A., Siebert, U.,
606 Madsen, P. T., & Teilmann, J. (2019). Long-term sound and movement

607 recording tags to study natural behavior and reaction to ship noise of seals.
608 *Ecology and Evolution*, 9(5), 2588-2601.

609 Mitani, Y., Sato, K., Ito, S., Cameron, M. F., Siniff, D. B., & Naito, Y. (2003). A
610 method for reconstructing three-dimensional dive profiles of marine
611 mammals using geomagnetic intensity data: results from two lactating
612 Weddell seals. *Polar Biology*, 26(5), 311–317.

613 Pavlov, V. V., Wilson, R. P., & Lucke, K. (2007). A new approach to tag design
614 in dolphin telemetry: Computer simulations to minimise deleterious effects.
615 *Deep-Sea Research Part II: Topical Studies in Oceanography*, 54(3–4),
616 404–414.

617 Pavlov, V. V., & Rashad, A. M. (2012). A non-invasive dolphin telemetry tag:
618 Computer design and numerical flow simulation. *Marine Mammal Science*,
619 28(1), 16–27.

620 Pennycuik, C. J., Fast, P. L. F., Ballerstädt, N., & Rattenborg, N. (2012). The
621 effect of an external transmitter on the drag coefficient of a bird's body, and
622 hence on migration range, and energy reserves after migration. *Journal of*
623 *Ornithology*, 153(3), 633–644.

624 Portugal, S. J., & White, C. R. (2018). Miniaturisation of biologgers is not
625 alleviating the 5% rule. *Methods in Ecology and Evolution*, 1(1), 1–2.

626 R Core Team. (2018). *R: A Language and Environment for Statistical*
627 *Computing*. R Foundation for Statistical Computing, Vienna. URL
628 <http://www.R-project.org>

- 629 Ropert-Coudert, Y., Knott, N., Chiaradia, A., & Kato, A. (2007). How do different
630 data logger sizes and attachment positions affect the diving behaviour of
631 little penguins? *Deep-Sea Research Part II: Topical Studies in*
632 *Oceanography*, 54(3–4), 415–423.
- 633 Ropert-Coudert, Y., Bost, C., Handrich, Y., Bevan, R. M., Butler, P. J., Woakes,
634 A. J., & Le Maho, Y. (2000). Impact of Externally Attached Loggers on the
635 Diving Behaviour of the King Penguin. *Physiological and Biochemical*
636 *Zoology*, 73(4), 438–444.
- 637 Roquet, F., Boehme, L., Block, B., Charrassin, J.-B., Costa, D., Guinet, C., ...
638 Fedak, M. A. (2017). Ocean Observations Using Tagged Animals.
639 *Oceanography*, 30(2), 139–139.
- 640 Rosen, D. A. S., Gerlinsky, C. G., & Trites, A. W. (2017). Telemetry tags
641 increase the costs of swimming in northern fur seals, *Callorhinus ursinus*.
642 *Marine Mammal Science*, 1–18.
- 643 Shepard, E., Wilson, R., Quintana, F., Gómez Laich, A., Liebsch, N., Albareda,
644 D., ... McDonald, D. (2008). Identification of animal movement patterns
645 using tri-axial accelerometry. *Endangered Species Research*, 10, 47–60.
- 646 Shorter, A., Murray, M., Johnson, M., Moore, M., & Howle, L. (2014). Drag of
647 suction cup tags on swimming animals: Modeling and measurement.
648 *Marine Mammal Science*, 30(2), 726–746.
- 649 Shorter, A., Shao, Y., Ojeda, L., Barton, K., Rocho-Levine, J., van der Hoop, J.,
650 & Moore, M. (2017). A day in the life of a dolphin: Using bio-logging tags for

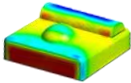
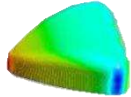
- 651 improved animal health and well-being. *Marine Mammal Science*, 33(3),
652 785–802.
- 653 Stidsholt, L., Johnson, M., Beedholm, K., Jakobsen, L., Kugler, K., Brinkløv, S.,
654 ... Madsen, P. T. (2018). A 2.6-g sound and movement tag for studying the
655 acoustic scene and kinematics of echolocating bats. *Methods in Ecology
656 and Evolution*, 10(1), 48-58.
- 657 Stimpert, A. K., Mattila, D., Nosal, E. M., & Au, W. W. L. (2013). Tagging young
658 humpback whale calves: Methodology and diving behavior. *Endangered
659 Species Research*, 19(1), 11–17.
- 660 Suliman, M. A., Mahmoud, O. K., Al-Sanabawy, M. A., & Abdel-Hamid, O. E.
661 (2009). Computational investigation of base drag reduction for a projectile
662 at different flight regimes. *Paper: ASAT-13-FM-05, 13th International
663 Conference on Aerospace Science and Aviation Technology, Military
664 Technical College, Kobry Elkobbah, Cairo, Egypt.*
- 665 Thorstad, E. B., Okland, F., & Heggberget, T. G. (2001). Are long term negative
666 effects from external tags underestimated? Fouling of an externally
667 attached telemetry transmitter. *Journal of Fish Biology*, 59(4), 1092–1094.
- 668 Tomotani, B. M., Bil, W., Jeugd, H. P., Pieters, R. P. M., & Muijres, F. T. (2019).
669 Carrying a logger reduces escape flight speed in a passerine bird, but
670 relative logger mass may be a misleading measure of this flight
671 performance detriment. *Methods in Ecology and Evolution*, 10(1), 70–79.
- 672 Treasure, A., Roquet, F., Ansoorge, I. J., Bester, M., Boehme, L., Bornemann,

- 673 H., ... de Bruyn, P. J. N. (2017). Marine mammals exploring the oceans
674 pole to pole: A review of the MEOP Consortium. *Oceanography*, 30(2),
675 132–138.
- 676 Tudorache, C., Burgerhout, E., Brittijn, S., & Van Den Thillart, G. (2014). The
677 effect of drag and attachment site of external tags on swimming eels:
678 Experimental quantification and evaluation tool. *PLoS ONE*, 9(11), 1–10.
- 679 Tyagi, A., & Sen, D. (2006). Calculation of transverse hydrodynamic coefficients
680 using computational fluid dynamic approach. *Ocean Engineering*, 33, 798–
681 809.
- 682 van der Hoop, J. M., Fahlman, A., Hurst, T., Rocho-Levine, J., Shorter, K. A.,
683 Petrov, V., & Moore, M. J. (2014). Bottlenose dolphins modify behavior to
684 reduce metabolic effect of tag attachment. *Journal of Experimental Biology*,
685 217(23), 4229–4236.
- 686 van der Hoop, J. M., Fahlman, A., Shorter, K. A., Gabaldon, J., Rocho-Levine,
687 J., Petrov, V., & Moore, M. J. (2018). Swimming Energy Economy in
688 Bottlenose Dolphins Under Variable Drag Loading. *Frontiers in Marine*
689 *Science*, doi:10.3389/fmars.2018.00465
- 690 Vandenabeele, S., Grundy, E., Friswell, M., Grogan, A., Votier, S., & Wilson, R.
691 (2014). Excess baggage for birds: Inappropriate placement of tags on
692 gannets changes flight patterns. *PLoS ONE*, 9(3).
- 693 Vandenabeele, S. P., Shepard, E. L. C., Grémillet, D., Butler, P. J., Martin, G.
694 R., & Wilson, R. P. (2015). Are bio-telemetric devices a drag? Effects of

- 695 external tags on the diving behaviour of great cormorants. *Marine Ecology*
696 *Progress Series*, 519, 239–249.
- 697 Vassberg, J. C., Tinoco, E. N., Mani, M., Rider, B., Zickuhr, T., Levy, D. W., ...
698 Murayama, M. (2014). Summary of the Fourth AIAA Computational Fluid
699 Dynamics Drag Prediction Workshop. *Journal of Aircraft*, 51(4), 1070–
700 1089.
- 701 Watson, K. P., & Granger, R. A. (1998). Hydrodynamic effect of a satellite
702 transmitter on a juvenile green turtle (*Chelonia mydas*). *Journal of*
703 *Experimental Biology*, 201(17), 2497–2505.
- 704 Williams, T.M. (2018). Swimming. In *Encyclopedia of marine mammals* (pp.
705 970-979). Academic Press.
- 706 Wilson, R. P., Holton, M., Wilson, V. L., Gunner, R., Tysse, B., Wilson, G. I., ...
707 Scantlebury, D. M. (2018). Towards informed metrics for examining the role
708 of human-induced animal responses in tag studies on wild animals.
709 *Integrative Zoology*, 14(1), 17-29.
- 710 Wilson, Rory P., & McMahon, C. R. (2006). Measuring devices on wild animals:
711 What constitutes acceptable practice? *Frontiers in Ecology and the*
712 *Environment*, 4(3), 147–154.
- 713

714 **Tables**

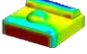
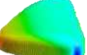
715 Table 1. The dimensions, volume, drag coefficient (C_d) (mean \pm standard deviation) and
 716 percentage increase in C_d over the baseline case (seal with no tag) (mean \pm standard
 717 deviation) of tag designs A and B. Means and percentage increase of drag are calculated
 718 over the range of positions tested (1-9).

Tag	Form	Dimensions (L x W x H; cm)	Volume (cm ³)	Drag coefficient (C_d) (mean \pm SD)	Drag coefficient % increase over the baseline (no tag) case (mean \pm SD)
A		10 x 7 x 4	280	0.075 \pm 0.002	27.4 \pm 4.2
B		11 x 10 x 4	440	0.064 \pm 0.001	8.9 \pm 1.8

719

Optimising biologging tags for minimal drag

720 Table 2. The drag force (N), power requirement (W), drag coefficient (C_d), and percentage increase of C_d over
 721 baseline case (seal with no tag), across all positions. Note that negative C_d values equates to downforce.
 722 Results shown are for the simulations at 5 ms^{-1} but apply equally across all swim speeds tested (see Methods).

	Tag	Position	Position (mm)	Drag (N)	Power (W)	Drag coefficient (C_d)	C_d increase over baseline case (seal with no tag) (%)	C_d (N)
	None	NA	NA	101.3	506.6	0.0588	NA	0.0
	A	1	215.75	125.1	625.5	0.0726	23.5	0.0
	A	2	325.37	122.5	612.3	0.0711	20.9	0.0
	A	3	411.47	127.0	635.0	0.0737	25.3	0.0
	A	4	580.60	132.5	662.6	0.0769	30.8	0.0
	A	5	667.69	133.8	669.1	0.0777	32.1	0.0
	A	6	783.83	133.9	669.5	0.0777	32.1	0.0
	A	7	900.90	131.7	658.3	0.0764	29.9	0.0
	A	8	968.21	130.6	653.1	0.0758	28.9	-0.0
	A	9	1083.44	125.1	625.5	0.0726	23.5	-0.0
	B	1	215.75	108.4	542.1	0.0629	7.0	-0.0
	B	2	325.37	109.8	548.8	0.0637	8.3	0.0
	B	3	411.47	112.0	560.0	0.0650	10.5	0.0
	B	4	580.60	113.4	566.9	0.0658	11.9	0.0
	B	5	667.69	112.0	560.0	0.065	10.5	-0.0
	B	6	783.83	111.3	556.6	0.0646	9.9	-0.0
	B	7	900.90	109.8	548.8	0.0637	8.3	0.0
	B	8	968.21	108.9	544.5	0.0632	7.5	0.0
	B	9	1083.44	107.9	539.4	0.0626	6.5	0.0